

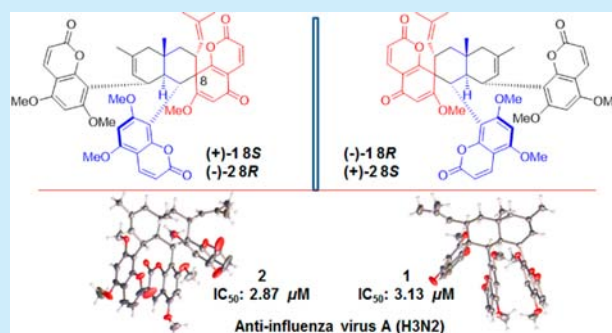
# Antiviral Spirotriscoumarins A and B: Two Pairs of Oligomeric Coumarin Enantiomers with a Spirodienone–Sesquiterpene Skeleton from *Toddalia asiatica*

Zhong-Hai Tang,<sup>†</sup> Yun-Bao Liu,<sup>†</sup> Shuang-Gang Ma,<sup>†</sup> Li Li, Yong Li, Jian-Dong Jiang, Jing Qu,<sup>\*</sup> and Shi-Shan Yu<sup>\*</sup>

State Key Laboratory of Bioactive Substance and Function of Natural Medicines, Institute of Materia Medica, Chinese Academy of Medical Sciences and Peking Union Medical College, Beijing 100050, China

## S Supporting Information

**ABSTRACT:** Two pairs of oligomeric coumarin enantiomers, spirotriscoumarin A [(+)-1 and (–)-1] and spirotriscoumarin B [(+)-2 and (–)-2], with a spirodienone–sesquiterpene fused skeleton were isolated from *Toddalia asiatica*. Their structures were unambiguously established using spectroscopic data, X-ray diffraction analysis, and the electronic circular dichroism (ECD) method. The racemic mixtures (±)-1 and (±)-2 exhibit 3-to-6-fold stronger antiviral activity against influenza virus A (H3N2) (IC<sub>50</sub>: 3.13 and 2.87 μM, respectively) than their corresponding optically pure enantiomers.



Oligomeric natural products, in which a secondary metabolite building block combines with itself at least three times (trimers), generally possess a great variety and complexity of architectures. The oligomers might form in serial or nonserial modes according to Snyder's classification,<sup>1</sup> and they have attracted widespread interest from synthetic chemists and resulted in a number of elegant total syntheses.<sup>1,2</sup> In addition, spirodienone-borne natural products represent another type of fascinating structure.<sup>3–5</sup> Spirodienones forming upon a specific structural skeleton by fusing with additional fragments and/or rings will lead to more complex structures. Typical examples of such molecules include the first antifungal drug, griseofulvin, and the antiprotozoal lead, aculeatin A.<sup>3–5</sup> Considering the importance of both the individual oligomer and spirodienone, the spirodienone–hybrid oligomers are expected to attract more attention from both chemists and biologists.

*Toddalia asiatica* (L.) Lam. (Rutaceae), a medicinal plant that is widely distributed in China, Japan, India, and Africa, has been applied as a folk medicine for treating colds, pyogenic infections, malaria, rheumatic arthritis, and traumatic injury.<sup>6,7</sup> *T. asiatica* primarily contains diversified coumarins (particularly prenylated and geranylated coumarins) and phenanthridine alkaloids.<sup>6,7</sup> Chemical screening of the extract of *T. asiatica* by LC–(+)-ESI–MS<sup>n</sup> revealed that two HPLC peaks had the characteristic UV absorption of coumarin with an unexpectedly high molecular weight at *m/z* 803 [M + H]<sup>+</sup> [Chart 1 in the Supporting Information], indicating the possibility of oligomeric coumarins. Structure-guided fractionation and purification led to the isolation of two pairs of nonserially produced

triscoumarin enantiomers, spirotriscoumarin A [(+)-1 and (–)-1] and spirotriscoumarin B [(+)-2 and (–)-2] (Figure 1).

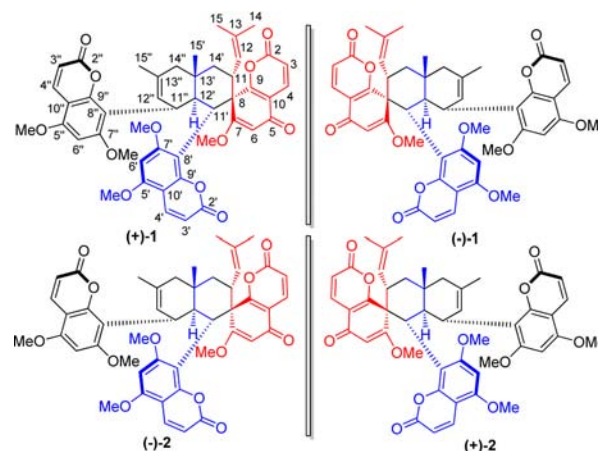


Figure 1. Structures of (+)-1, (–)-1, (+)-2, and (–)-2.

Compounds 1 and 2 not only feature the first spirodienone–sesquiterpene fused skeleton but also the most complex oligomeric coumarin. Moreover, 1 and 2 are two pairs of enantiomers: (±)-1 and (±)-2. Chiral separation and electronic circular dichroism (ECD) calculations led to the assignment of each optically pure enantiomer as (+)-1, (–)-1, (+)-2, and

Received: August 30, 2016

Published: September 27, 2016

(-)-2. Notably, (+)-1/(-)-2 and (-)-1/(+)-2 are also two pairs of diastereomers at spiro carbon C-8. Subsequently, we proposed a pathway of nonsesquiterpene origin for the biosynthesis of the two coumarin–sesquiterpene-like hybrids (**1** and **2**) in which two steps of [4 + 2] Diels–Alder cycloadditions may be involved.<sup>8</sup>

The racemic mixtures ( $\pm$ )-**1** and ( $\pm$ )-**2** and optically pure enantiomers (+)-**1**, (-)-**1**, (+)-**2**, and (-)-**2** were tested for their inhibition of influenza virus A. Notably, the racemic mixtures ( $\pm$ )-**1** and ( $\pm$ )-**2** exhibited 3-to-6-fold stronger antiviral activity against influenza virus (H3N2) (IC<sub>50</sub>: 3.13 and 2.87  $\mu$ M, respectively) than their corresponding pure enantiomers (+)-**1**, (-)-**1**, (+)-**2**, and (-)-**2**.

Herein, we report the isolation, chiral separation, structural elucidation, biosynthetic consideration, and antiviral evaluation of spirotriscoumarins **A** and **B**.

Compound **1** was obtained as a colorless crystal (in CHCl<sub>3</sub>–MeOH) and was determined to have a molecular formula of C<sub>47</sub>H<sub>46</sub>O<sub>12</sub> with 25 degrees of unsaturation based on its HR-ESIMS [M + H]<sup>+</sup> *m/z* 803.3063 and interpretation of its NMR data. The <sup>1</sup>H NMR spectrum (Table S1 and Figure S6 in the SI) presented signals for three pairs of *cis* olefinic protons ( $\delta_{\text{H}}$  5.45–7.65 ppm); three singlet aromatic protons at  $\delta_{\text{H}}$  5.99, 5.97, and 5.17 ppm; five methoxy groups at  $\delta_{\text{H}}$  4.07, 3.96, 3.72  $\times$  2, and 3.57 ppm; and four methyl groups at  $\delta_{\text{H}}$  1.64, 1.53, 1.47, and 1.36 ppm. Analysis of the <sup>1</sup>H and <sup>13</sup>C NMR data (Tables S1 and S2 in the SI) with the aid of a DEPT experiment revealed the presence of 4 carbonyls (one ketone carbonyl at  $\delta_{\text{C}}$  182.9), 26 olefinic carbons, 4 methyls, 5 methoxys, 2 methylenes, 4 methines, and 2 sp<sup>3</sup> quaternary carbons ( $\delta_{\text{C}}$  55.6 and 36.0). Detailed analysis of the 1D and 2D NMR data allowed for the assignment of four partial structures, I–IV (Figure 2), for **1**.

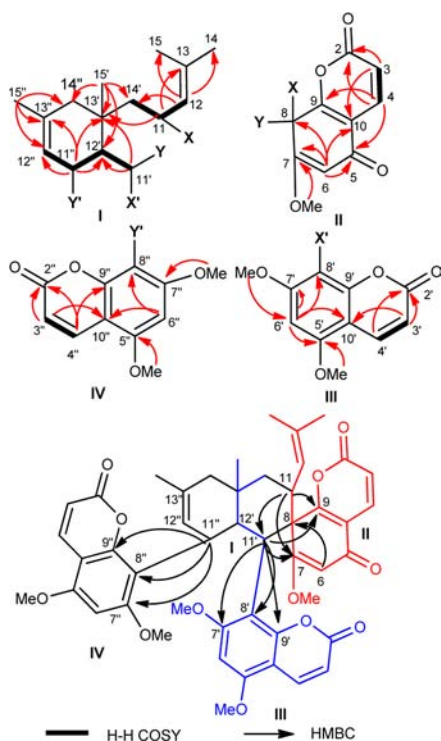


Figure 2. COSY and HMBC correlations of **1**.

Partial structure **I** was established to be a sesquiterpene moiety based on the spin systems C(14')H<sub>2</sub>–C(11)H–C(12)H and C(11')H–C(12')H–C(11'')H–C(12'')H assigned by COSY and HSQC, together with HMBC correlations of H-12/C-14, C-15, and C-14'; H-11/C-13 and C-13'; H-15'/C-14', C-14'', and C-12'; H-15''/C-14'', and C-12''; and H-11''/C-13'' and C-13'. Partial structures **III** and **IV** were easily established to be two typical coumarin units based on their COSY and HMBC correlations. However, partial structure **II**, a spirodienone coumarin unit differing from the typical coumarin aryl-substitution pattern, was determined on the basis of the three protons at  $\delta_{\text{H}}$  7.55 (1H, d, *J* = 9.5 Hz), 6.20 (1H, d, *J* = 9.5 Hz), and 5.17 (1H, s); one ketone carbon at  $\delta_{\text{C}}$  182.8; one lactone carbon at 160.2; and HMBC correlations of H-3/C-10 and C-2; H-4/C-2, C-9 and C-5 (ketone carbon); H-6/C-8 (sp<sup>3</sup> quaternary carbon) and C-10; and OMe-7/C-7.

Partial structures **I** and **II** were confirmed to be fused through C8–C11 and C8–C11' to form a spirodienone structure based on the HMBC correlations from H-11/H-11' to C-7/C-9. The HMBC correlations from H-11' to C-7'/C-8'/C-9' led to the assignment of the connectivity of partial structures **I** and **III** through C11'–C8'. Similarly, the connectivity of partial structures **I** and **IV** was established to be through C11''–C8'' based on the HMBC correlations from H-11'' to C-7''/C-8''/C-9''. Thus, the planar structure of **1** was established and named spirotriscoumarin **A**.

The relative configurations were determined by NOE correlations (Figure 3, Figures S12 and S13 in the SI). The

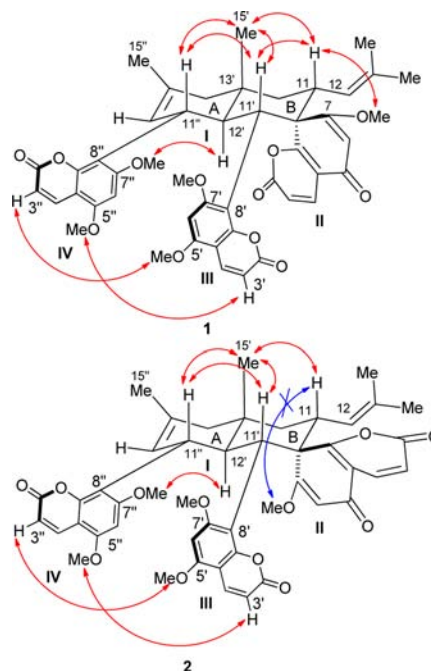


Figure 3. Key NOE correlations of compounds **1** and **2**.

NOE correlations of H-11/H<sub>3</sub>-15', H-11/H-11', H-11'/H-11'', H-11''/H<sub>3</sub>-15', and H-11''/H<sub>3</sub>-15' confirmed that H-11, H-11', H-11'', and Me-15' were all axial protons ( $\beta$ -orientated). Thus, rings **A** and **B** were trans-fused, indicating that H-12' must be in an opposite axial orientation ( $\alpha$ -H) and that bonds C11–C12, C8'–C11', and C8''–C11'' were in the equatorial orientations. The NOE correlation between the axial H-11 and 7-OMe allowed for the assignment of the relative configuration of the

spirodienone functionality. The  $\alpha$ -oriented axial H-12' showed a NOE correlation with 7''-OMe, indicative of the  $\alpha$ -oriented aryl unit (C5''–C9'') and  $\beta$ -oriented lactone unit (C2''–C4'') of partial structure IV. The NOE correlations of OMe-5''/H-3' and OMe-5'/H-3'' revealed that the orientation of partial structure III was opposite that of partial structure IV. Thus, the relative configuration of **1** was identified as shown in Figure 3.

Single-crystal X-ray diffraction of **1** using Cu K $\alpha$  radiation (Figure 4) confirmed the proposed planar structure and the

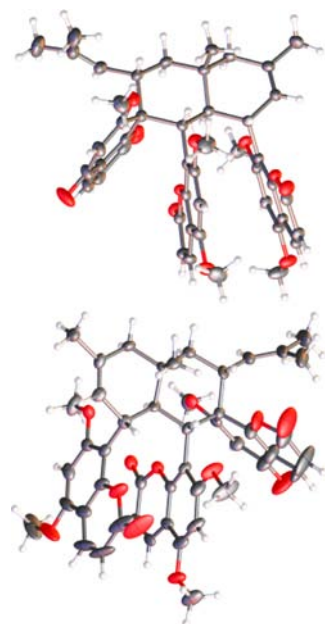


Figure 4. X-ray crystal structures of **1** (up) and **2** (down).

relative configuration deduced by the NOE experiments. Crystallographic data have been deposited at the Cambridge Crystallographic Data Centre and allocated the deposition no. CCDC 1442570. Note that the crystals of **1** have the space group *P*-1, indicating a racemic nature, as also evidenced by the lack of optical activity. Compound ( $\pm$ )-**1** was then successfully separated via chiral HPLC to two optically pure enantiomers: (+)- and (–)-**1**, respectively (Figure S1 in the SI).

The absolute configurations of individual (+)- and (–)-**1** were determined by comparison of their experimental and calculated ECD spectra.<sup>9</sup> The theoretical ECD spectra of model compounds **1a** and **1b** (Figure S14 in the SI) were mirror images and matched well with the experimental ECD spectra of (+)- and (–)-**1**, respectively (Figure S28 in the SI). Thus, the absolute configurations of (+)- and (–)-**1** were assigned as (8*S*,11*R*,11'*S*,12'*R*,13'*S*,11''*R*)-spirotriscoumarin **A** and (8*R*,11*S*,11'*R*,12'*S*,13'*R*,11''*S*)-spirotriscoumarin **A**, respectively.

Compound **2** was obtained as a colorless crystal. Its molecular formula, C<sub>47</sub>H<sub>46</sub>O<sub>12</sub>, as deduced from HRESIMS, was identical to that of **1**. The UV, IR, CD, and NMR spectral data of **2** also resembled those of **1**. Careful analysis of the spectroscopic data allowed us to conclude that its planar structure was identical to that of **1**.

NOE correlations (Figure S26 in the SI) of H-11/H<sub>3</sub>-15', H-11/H-11', H-11'/H-11'', H-11'/H<sub>3</sub>-15'', and H-11''/H<sub>3</sub>-15' indicated that the relative configuration of H-11/H-11'/H-11''/H<sub>3</sub>-15'' in **2** was same as that in **1**. NOE correlations of OMe-5'/H-3'' and OMe-5''/H-3' (Figure S27 in the SI)

indicated that the relative configuration of partial structures III and IV were as shown and identical to that of **1**. The <sup>13</sup>C NMR chemical shifts of **2** were nearly identical to those of **1** except the carbons (C-7, C-9, C-11, and C-11') directly connected with the spiro carbon C-8. The <sup>13</sup>C NMR data of C-7/C-11' and C-9/C-11 in **2** downshifted 2.9/1.3 ppm and upshifted 1.2/0.9 ppm compared with **1**, respectively, indicating that **2** could be a C-8 diastereomer of **1**. However, the relative configuration of the remaining spiro carbon C-8 could not be directly determined on the basis of the available NOE data. Fortunately, a single-crystal X-ray diffraction experiment was successfully performed to confirm the proposed planar structure and the relative configuration of C-11, C-11', C-12', C-13', and C-11'' deduced by NOE experiments, and this experiment also revealed that the relative configuration of partial structure II attached at spiro C-8 in **2** was opposite to that in **1** (Figure 3 and Figure S27 in the SI).

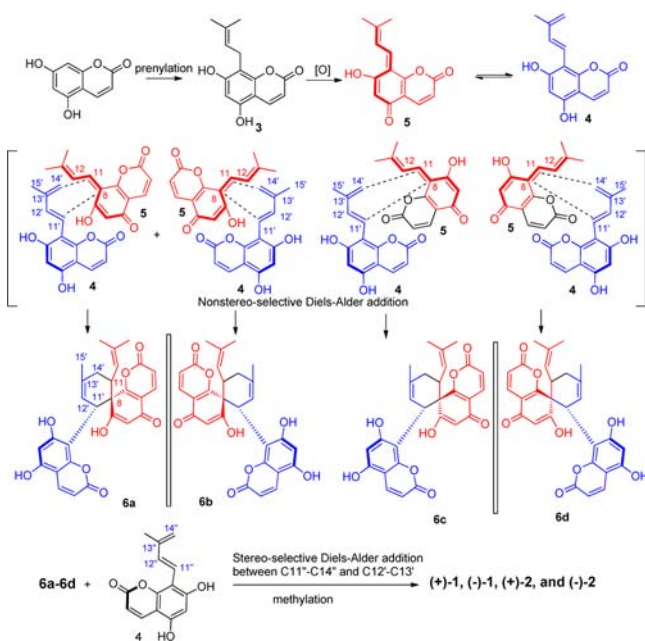
The X-ray diffraction experiment (CCDC no. 1442569, Table S4 in the SI) clearly showed that **2** was also a pair of enantiomers, similar to **1**, with the space group *Pbnc*. As for **1**, the enantiomers of **2** were chirally separated and subjected to ECD calculations. The theoretical ECD spectra of model compounds **2a** and **2b** (Figure S28 in the SI) were also mirror images and matched well with the experimental ECD spectra of (+)- and (–)-**2**, respectively (Figure S14 in the SI). Thus, the absolute configurations of (+)- and (–)-**2** were assigned as (8*S*,11*S*,11'*R*,12'*S*,13'*R*,11''*S*)-spirotriscoumarin **B** and (8*R*,11*R*,11'*S*,12'*R*,13'*S*,11''*R*)-spirotriscoumarin **B**, respectively.

Structurally, **1** and **2** are trimeric coumarins that possess a spirodienone–sesquiterpene hybrid skeleton with six chiral centers at C-8, C-11, C-11', C-12', C-13', and C-11''. Compounds **1** and **2** were formed in a nonserial mode and added new members to the oligomeric natural products.<sup>1</sup> The spirodienone–sesquiterpene hybrid skeleton further enhanced the novelty and complexity of the oligomers.<sup>1,2</sup>

Biosynthetically, the cyclic sesquiterpene moiety is normally derived from the fundamental precursor farnesyl diphosphate (FPP), which is generally synthesized via the addition of a C5 IPP unit to GPP in an extension of the GPP synthase reaction.<sup>10</sup> However, in the cases of **1** and **2**, the sesquiterpene moiety may not be of sesquiterpene origin based on their structures. Hence, a possible biosynthetic pathway for **1** and **2** was proposed (Scheme 1). The possible biosynthetic monomeric precursor **3**,<sup>11</sup> the prenylated coumarin, may be converted to intermediate **5** through dehydration and oxidation reactions. Subsequently, nonstereoselective Diels–Alder addition of **5** with intermediate **4** would afford **6a–d**. Due to the steric hindrance of the substitution unit (substructure III) at C-11', a stereoselective Diels–Alder addition between **6a–d** and **4** could occur.<sup>8</sup> Finally, full methylation will lead to the production of (+)-**1**, (–)-**1**, (+)-**2**, and (–)-**2**. When compounds **1** and **2** were obtained from the plant, we also doubted that they could be artifacts. We attempted to synthesize **1** and **2** starting from the proposed intermediate **4** by using the chemical conditions for Diels–Alder addition but failed.

Influenza remains a serious risk to human lives worldwide. Increasing the availability of new anti-influenza drugs or discovering novel anti-influenza leads will provide us with better approaches for controlling influenza and will have a positive impact on disease control.<sup>12</sup> Therefore, following the racemic resolution and the determination of the absolute

**Scheme 1. Plausible Biosynthetic Pathway of (+)-1, (–)-1, (+)-2, and (–)-2**



configuration of each enantiomer, the next step was evaluating the influenza virus A activity of two racemic mixtures, ( $\pm$ )-1 and ( $\pm$ )-2, and four single enantiomers, (+)-1, (–)-1, (+)-2, and (–)-2.<sup>13</sup> As shown in Table S5 in the SI, the racemic mixture of ( $\pm$ )-1 and ( $\pm$ )-2 possessed strong activity against influenza virus A (H3N2) with IC<sub>50</sub> values of 3.13 and 2.87  $\mu$ M, respectively, the same inhibitory level as positive controls. The pure enantiomers, (+)-1, (–)-1, (+)-2, and (–)-2, exhibited 3- to 6-fold weaker activity against influenza virus A (IC<sub>50</sub>: 9.86, 11.11, 17.46, and 8.62  $\mu$ M, respectively) than their corresponding racemic mixtures ( $\pm$ )-1 and ( $\pm$ )-2. The bioassay data indicated that synergistic effects between (+)-1 and (–)-1 and between (+)-2 and (–)-2 against influenza virus A may exist.<sup>14,15</sup>

In conclusion, we discovered a new family of complex coumarin trimers with a spirodienone–sesquiterpene-like hybrid skeleton. Biosynthetically, these coumarin–sesquiterpene hybrids may derive from Diels–Alder addition between structurally simple prenylated coumarins rather than from typical sesquiterpene origin. Remarkably, each racemic mixture exhibited stronger antiviral activity than the corresponding pure enantiomer, suggesting that a synergistic effect occurred. The structural complexity and novelty and the interesting bioactivity data might attract considerable attention from synthetic chemists and biologists.

## ■ ASSOCIATED CONTENT

### Supporting Information

The Supporting Information is available free of charge on the ACS Publications website at DOI: 10.1021/acs.orglett.6b02572.

Detailed experimental procedures, 1D and 2D NMR, MS, and IR spectra and X-ray crystal data (PDF)

## ■ AUTHOR INFORMATION

### Corresponding Authors

\*E-mail: qujing@imm.ac.cn.

\*E-mail: yushishan@imm.ac.cn.

### Author Contributions

<sup>†</sup>Z.-H.T., Y.-B.L., and S.-G.M. contributed equally.

### Notes

The authors declare no competing financial interest.

## ■ ACKNOWLEDGMENTS

We are grateful to the Department of Instrumental Analysis of our institute for the measurements of UV, IR, NMR, and MS spectra and to the Analysis and Testing Center, Beijing University of Chemical Technology, for the X-ray crystallographic measurement and analysis. This work was supported by grants from the Natural Science Foundation of China (No. 21132009) and from the National Mega-project for Innovative Drugs (No. 2012ZX09301002-002).

## ■ REFERENCES

- (1) Snyder, S.; ElSohly, A.; Kontes, F. *Nat. Prod. Rep.* **2011**, *28*, 897–924.
- (2) Li, C.; Lei, X. *J. Org. Chem.* **2014**, *79*, 3289–3295.
- (3) Petersen, A.; Rønne, M.; Larsen, T.; Clausen, M. *Chem. Rev.* **2014**, *114*, 12088–12107.
- (4) Cacho, R.; Chooi, Y.; Zhou, H.; Tang, Y. *ACS Chem. Biol.* **2013**, *8*, 2322–2330.
- (5) Heilmann, J.; Mayr, S.; Brun, R.; Rali, T.; Sticher, O. *Helv. Chim. Acta* **2000**, *83*, 2939–2945.
- (6) Lin, T.; Huang, Y.; Tang, G.; Cheng, Z.; Liu, X.; Luo, H.; Yin, S. *J. Nat. Prod.* **2014**, *77*, 955–962.
- (7) Phatchana, R.; Yenjai, C. *Planta Med.* **2014**, *80*, 719–722.
- (8) Zhan, Z.; Ying, Y.; Ma, L.; Shan, W. *Nat. Prod. Rep.* **2011**, *28*, 594–629.
- (9) Shi, Y.; Liu, Y.; Li, Y.; Li, L.; Qu, J.; Ma, S.; Yu, S. *Org. Lett.* **2014**, *16*, 5406.
- (10) Dewik, P. *Medicinal Natural Products: A Biosynthetic Approach*, 3rd ed.; John Wiley & Sons: Chichester, U.K., 2009; pp 210.
- (11) Murray, R.; Jorge, Z. *Tetrahedron* **1984**, *40*, 3129–3132.
- (12) Palese, P. *Nat. Med.* **2004**, *10*, S82–S87.
- (13) Li, Y.; Shan, G.; Peng, Z.; Zhu, J.; Meng, S.; Zhang, T.; Gao, L.; Tao, R.; Li, Y.; Jiang, J.; Li, Z. *Antiviral Chem. Chemother.* **2010**, *20*, 259–268.
- (14) Batista, J. M., Jr.; Batista, A. N. L.; Rinaldo, D.; Vilegas, W.; Ambrósio, D. L.; Cicarelli, R. M. B.; Bolzani, V. S.; Kato, M. J.; Nafie, L. A.; López, S. N.; Furlan, M. *J. Nat. Prod.* **2011**, *74*, 1154–1160.
- (15) Shekh-Ahmad, T.; Mawasi, H.; McDonough, J.; Finnell, R.; Włodarczyk, B.; Yavin, E.; Bialer, M. *Epilepsia* **2014**, *55*, 1944–1952.